

Loi Do¹, Marc A Zempere^{2,3}, Haley E Wiskoski¹, Adam S Bernstein¹, Pradyumna Bharadwaj³, Natalie Carey^{2,3}, Christie Nguyen^{2,3}, Chidi Ugonna¹, Nan-kuei Chen¹, Gene E Alexander^{2,3}, Carol A Barnes^{2,3,4}, and Theodore P Trouard^{1,2}

1. Department of Biomedical Engineering, University of Arizona, Tucson, AZ, 85724 2. Evelyn F. McKnight Brain Institute, University of Arizona, Tucson, AZ 85724 3. Department of Psychology, University of Arizona, Tucson, AZ 85724 4. Departments of Neurology and Neuroscience, University of Arizona, Tucson



THE UNIVERSITY OF ARIZONA
COLLEGE OF ENGINEERING

Biomedical Engineering

Introduction

Animal models play an important role in preclinical and translational studies of the human brain. MRI, being both non-invasive and inherently translational, can play an important role in comparing brain anatomy in animals and humans. Furthermore, diffusion-weighted MRI (dMRI) can examine white matter connectivity and microstructural changes as a function of age. Characterization of volumes and structural integrity provide insight into the connectivity of different brain regions during both healthy cognitive aging and brains with various levels of cognitive aptitude.

In this study we used magnetic resonance imaging to characterize rat brains in healthy cognitive aging. The principal goals of the present study were to establish in rodent model:

1. Whether non-invasive volumetric MRI is a sensitive enough method to detect regional differences as a function of age and cognition.
2. Whether non-invasive dMRI is a sensitive enough method to detect white matter connectivity and microstructural changes as a function of age and cognition.

Methods

Male Fischer 344 rats (n=110) were acquired at young adult (6 months, n=49), middle aged (15 months, n= 35) and old adult (23 months, n= 26) ages. These animals underwent a battery of behavioral tasks, beginning with the Morris Watermaze (Figure 1) over 6 weeks resulting in each age group being sub-divided into 3 sub-groups of high, average and low cognition using corrected integrated path length (CIPL) score which utilized the last 12 spatial trails of the Morris Watermaze.

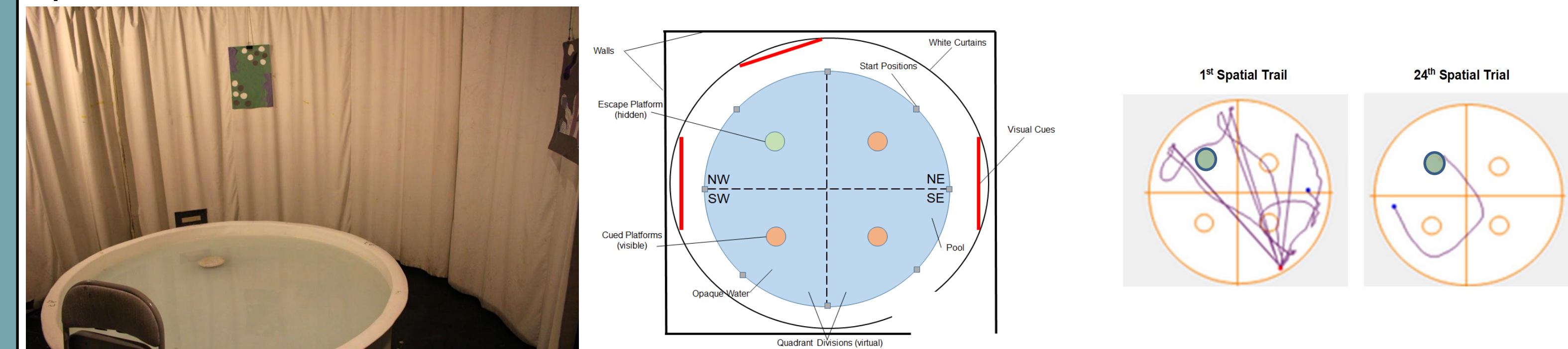


Figure 1. Morris Watermaze pool (left), schematic of the experiment pool and visual cues around the room (middle) and example of CIPL performance tracking of a rat during the first and final spatial trials (right) with the safety platform in the northwest quadrant.

At the end of the 6 weeks, body weights were measured and neurological imaging was carried out on a 7T Bruker Biospec (Bruker, Billerica, MA, Figure 2) MRI scanner. T2-weighted 3D Rapid Acquisition and Refocused Echoes data, were collected, with the following imaging parameters: matrix size=256x192x128, resolution=150 μ m TR=1500ms, ETL= 8, TE_{eff} = 40ms, time of acquisition=76 min. Diffusion-weighted single shot spin using echo echo planar imaging acquisition scheme was carried out with an in-plane resolution of 300X300 μ m and slice select dimension of 1mm and b=1000 s/mm² with 8 b=0s/mm² at 64 directions and repeated twice at b=2000 b=3000 (Figure 3).



Figure 2. Bruker small animal MRI scanner (left) and close up of cradle with 4 channel receiver coil (right) that was mounted on top of the animal's head for minimal distance from subject to receiver for minimal signal loss. During imaging animals are anesthetized with a mixture of oxygen and isoflurane delivered into the nose cone and the head is immobilized via bite bar, ear bars and the nose cone. Temperature, respiratory rate, O₂ sat and pulse are continuously monitored throughout the experiment using a variety of transducers.

Methods (Image Analysis)

Image processing of volumetric images (Figure 4) include brain extraction using a semi-automated process as well as bias correction due to non-uniform surface coil sensitivity using the ANTs software (2). A Fischer 344 T2-weighted template image (60 μ m isotropic voxel size) and labeled atlas (117 regions of the brain) (1) was used to perform the registration. The template image was registered to each individual animal in the study using linear and non-linear registration. The deformation fields produced from the registration were then applied to the 117-region labeled atlas and an in-house *MATLAB* code was used to calculate the volume of individual regions of interest (ROIs) in the brain. To compare ROI volumes across age and cognitive score, the volume of each ROI was normalized to total intracranial volume (TIV, 3).

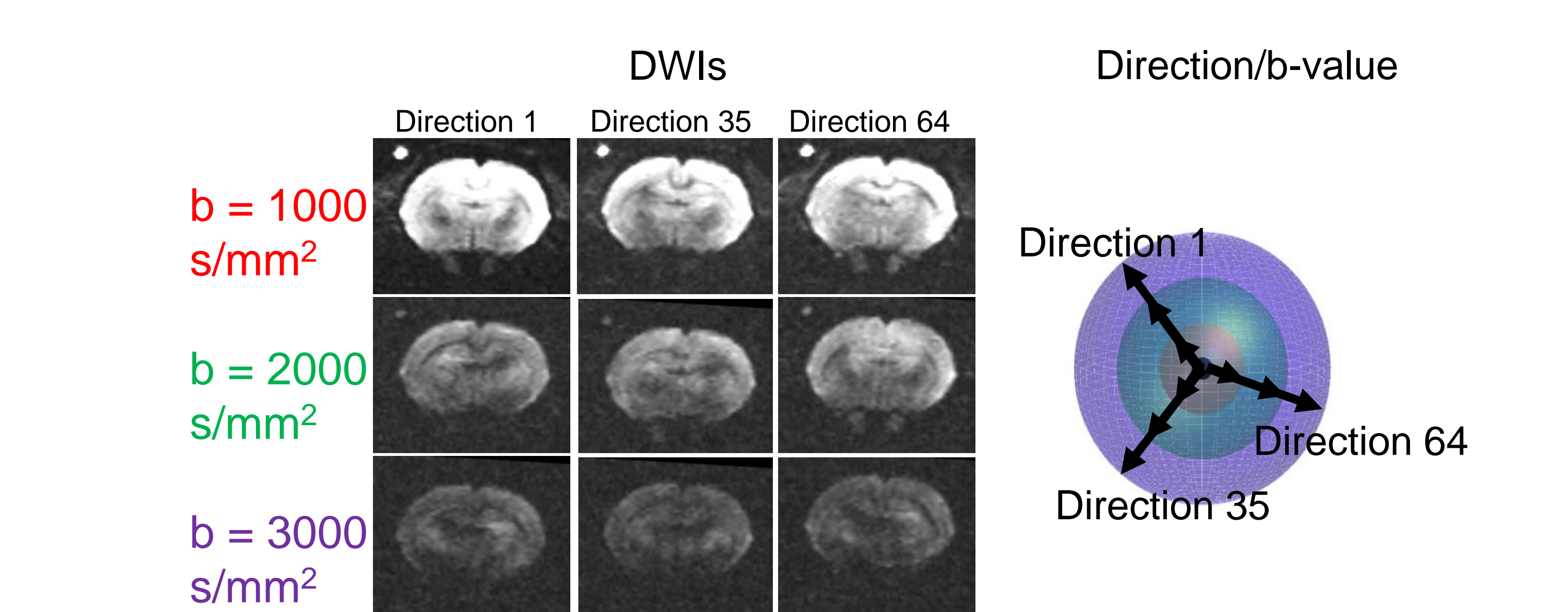


Figure 3. DMRI images (left) of a representative brain showing the 1 slice of the acquisition volume collected at 3 gradient strengths, namely b=1000, b=2000 and b=3000. The acquisition scheme (right) with the inner red shell representing b=1000, middle green shell representing b=2000 and outer purple shell representing b=3000. In each of the 3 shells 64 directions (x,y,z) are defined and at each direction an entire volume of the brain is acquired. Note that the signal to noise ratio of the images decreases as the b-value increases but better contrast is acquired at higher order b-values.

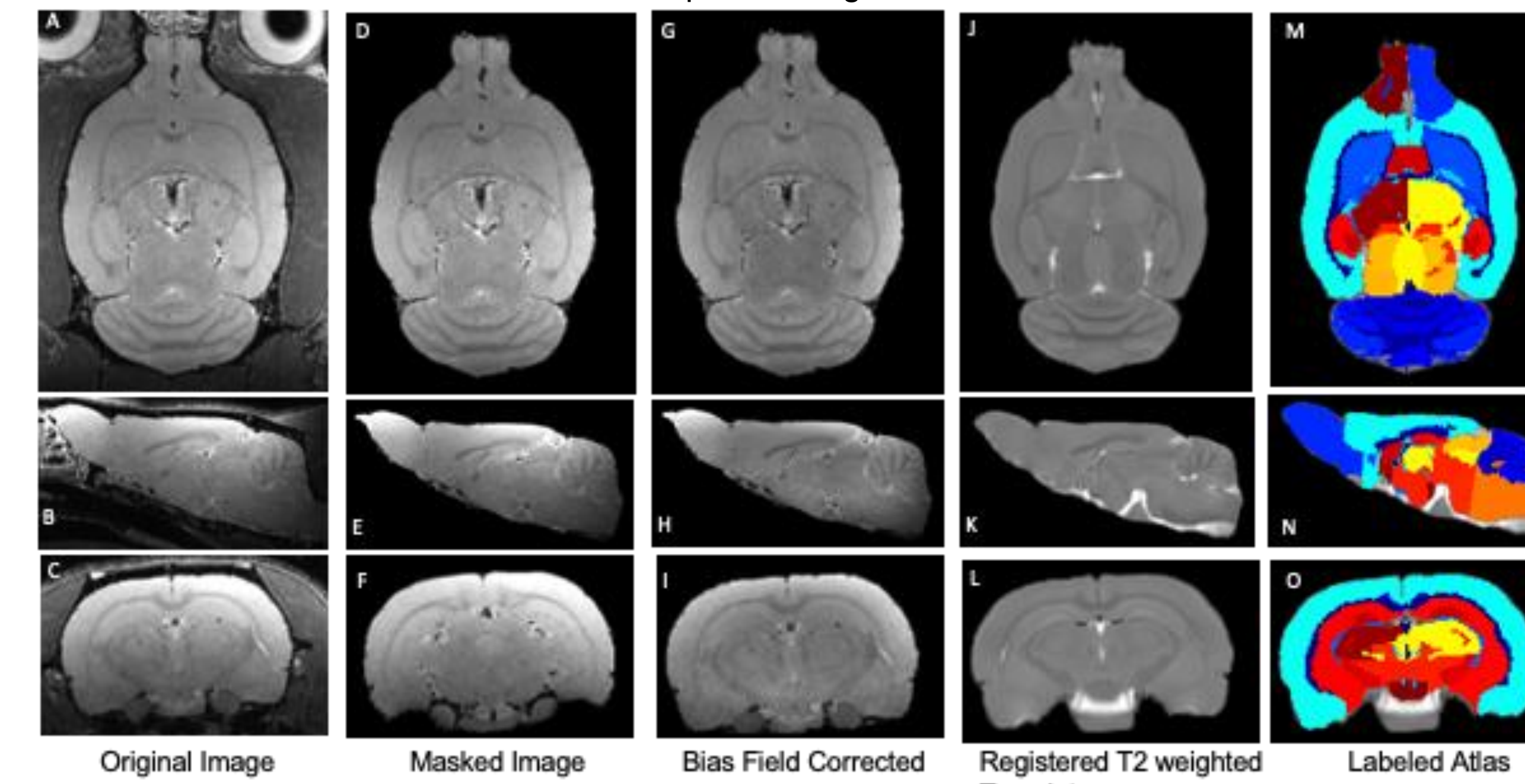


Figure 4. Processing pipeline is shown in 3 orthogonal views as the original (A,B,C) images undergo a brain extraction (D,E,F) and a bias correction for surface coil sensitivity (G,H,I). A T2-weighted template (J,K,L) is then registered to native space. The deformation field generated from this registration is then applied to an atlas (M,N,O) to bring the atlas to native space.

Results

Example images demonstrating the processing steps are shown in Figure 4. Global total brain volume calculated from semi-automatic brain extraction are plotted for each age group (Figure 5, left) shows a significant difference from young adult to middle age and young adult to old adult; however there is no significant difference between middle aged and old adult groups. Total hippocampal volume (Figure 5, middle) showed a statistically significant change in age but not cognition. There was no significant difference in fractional anisotropy (FA) of the corpus callosum, an important white matter tract, across age or cognitive status.

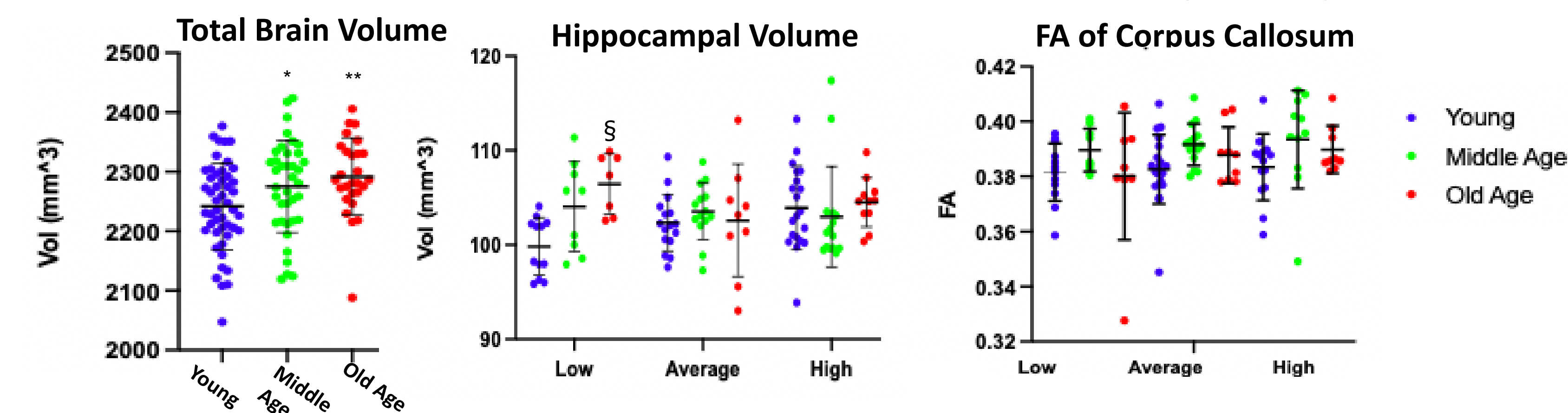


Figure 5. Global (left) volumetric comparison shows that the brain significantly increases in volume between 6 months and the two older age groups (middle aged and old age). Regional volumetric (middle) analysis of the hippocampus shows an effect of age but no effect of cognitive status. Microstructural fractional anisotropy (FA) comparisons of the corpus callosum (right) showed no significant difference in FA across age or cognitive groups. * Indicates p<0.05 compared with young. ** Indicates p<0.01 compared with young. § Indicates p<0.05 compared with young low group.

Diffusion-weighted MRI results were analyzed using both diffusion tensor imaging (DTI) and Fixel based analysis (FBA) frameworks. Figure 6 compares DTI ellipsoids to fiber orientation distribution (FOD) functions from the same representative animal. Fixels (fiber density elements) were calculated from FODs and are shown in Figure 7. Fixel data reveals changes in fiber density and significant differences in fiber density and cross sectional (FDC) area across age but not cognitive groups. Figure 7 shows voxels where there was a significant difference in FDC and in general older animals displayed higher values of FDC than younger animals.

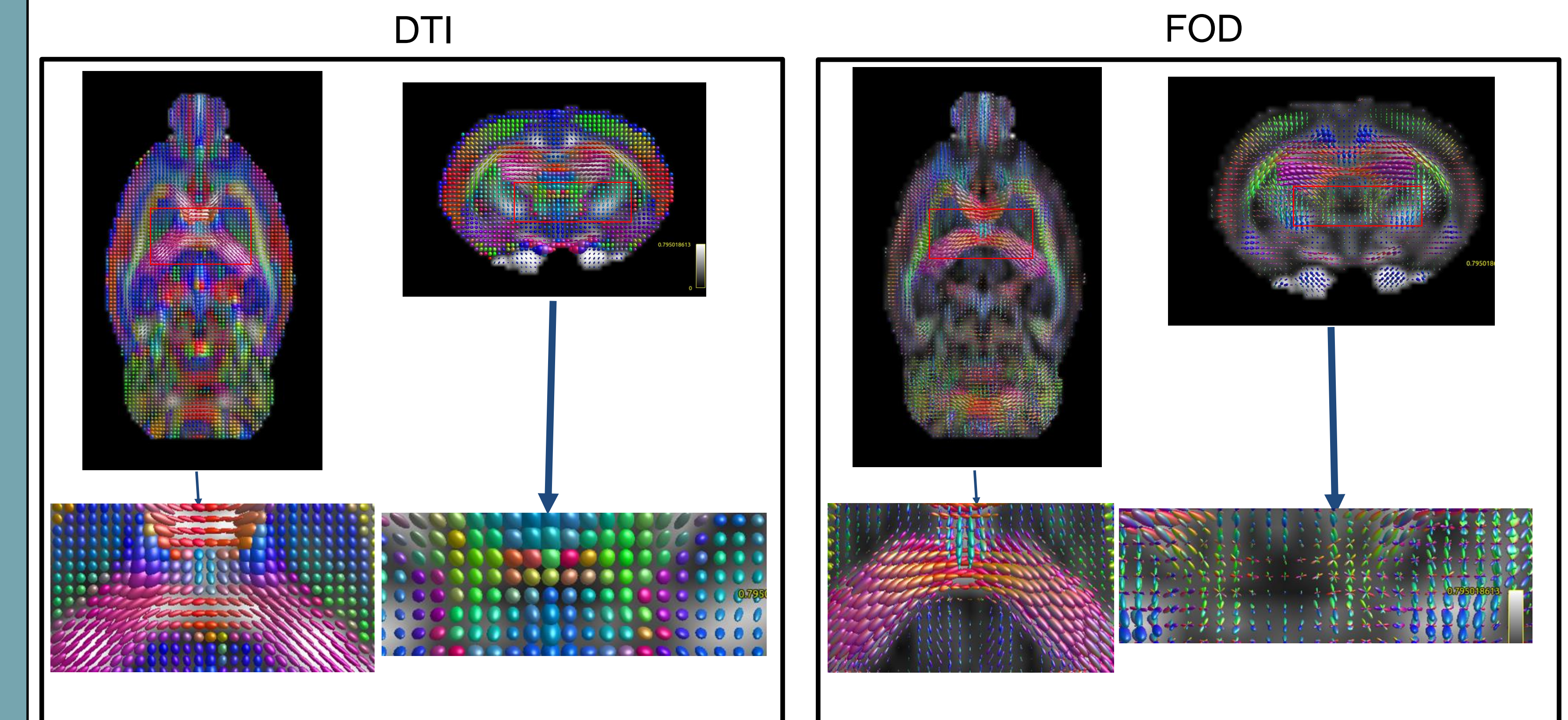


Figure 6. A single slice of diffusion tensor imaging (DTI, left block) and fiber orientation distribution (FOD, right block) of a representative rat brain shown in 2 orthogonal views. Zoomed in (bottom row) views show that the DTI gives voxel-wise data on the overall orientation of the fibers in a particular voxel, while FOD provides more detailed characterization of the fibers within each voxel, especially in regions known to have crossing fiber populations.

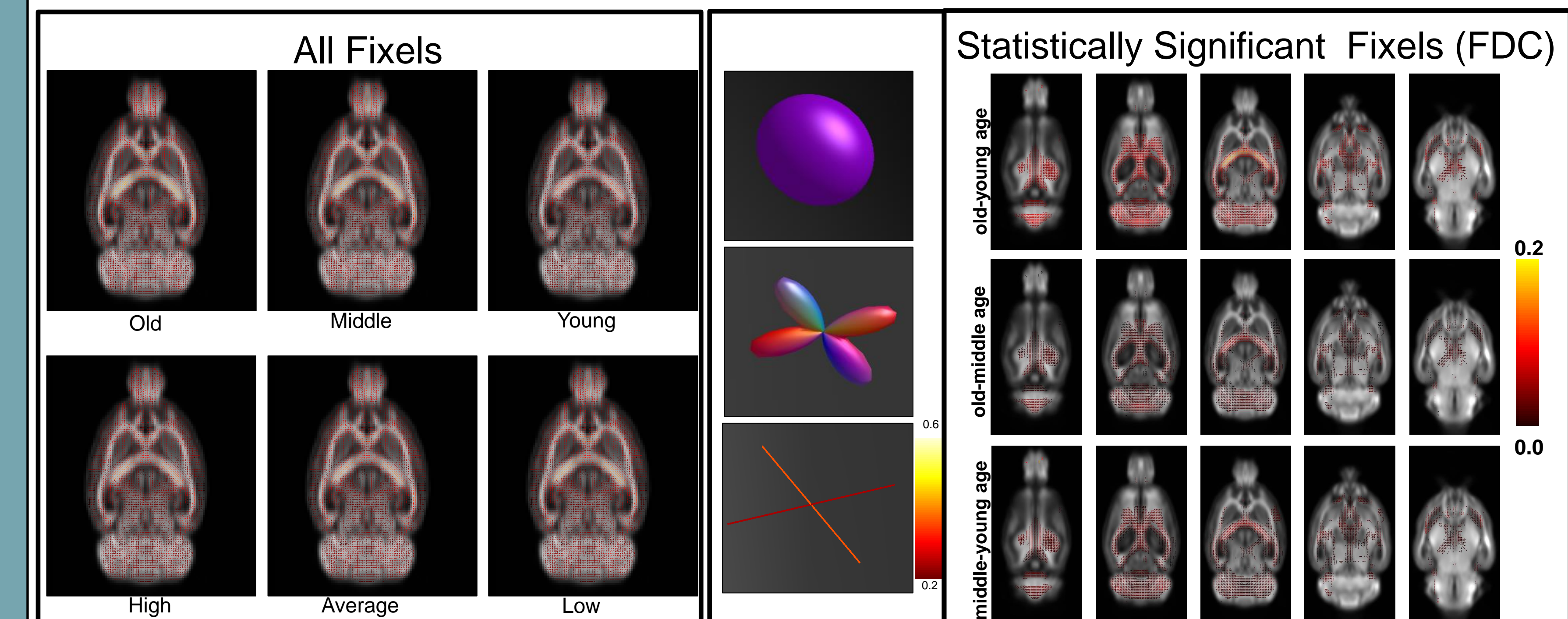


Figure 7. Fixel plots (left block) showing all fixels in a group averaged rat brain. They are grouped by age (top row) or cognitive group (bottom row). A representative voxel with crossing fibers (middle block) shows the DTI glyph (top), FOD glyph (middle) and fixels (bottom) within that voxel. Note that multiple fixels can exist in the same voxel if there are multiple crossing fiber populations. Multi-slice fixel plots (right block) showing difference maps of old-young age (top row), old-middle aged (middle row) and middle-young age (bottom row) are masked by p<0.05, i.e. all displayed fixels in this plot show statistically significance with respect to age. Fixel data reveals changes in FDC between groups and showed significant differences between age but not cognitive groups. Voxels where there was a significant difference in FDC is shown on the right block and in general older animals displayed higher values of FDC than younger animals.

Discussion

These data clearly indicate that the entire rat brain continues to grow between 6 and 15 months of age, but stabilized after 15 months, out to 23 months of age. For group-wise analysis considering different ages, total brain volume can, therefore, be a confounding variable that needs to be accounted for (3, 4). Specifically, when the hippocampus was measured independently, it also showed an increase across age in the low cognitive group, which is of particular interest because in human studies its decrease in volume has been shown to be an early indicator of potential pathological conditions. In contrast, FA showed no difference in age or across cognitive status in these same rats.

References

1. Goerzen, D., Fowler, C., Devenyi, G.A. et al. An MRI-Derived Neuroanatomical Atlas of the Fischer 344 Rat Brain. *Sci Rep* 10, 6952 (2020).
2. Avants BB, Yushkevich P, Pluta J. et al. The optimal template effect in hippocampus studies of diseased populations. *Neuroimage*. 2010 Feb 1;49(3):2457-66.
3. Barnes J, Ridgway GR, Bartlett J et al. Head size age and gender adjustment in MRI studies: a necessary nuisance? *Neuroimage*. 2010 Dec;53(4):1244-55.
4. McCutcheon JE and Marinelli M. Age matters *Eur J Neurosci*. 2009 Mar; 29(5): 997-1014.

Acknowledgements

NIH Grants RO1 AG049464, RO1 AG049465, McKnight Brain Research Foundation, and Biomedical Imaging and Spectroscopy Training Grant-5T32EB000809